Proc. Natl. Acad. Sci. USA
Vol. 84, pp. 6438–6442, September 1987
Biophysics

Structure of the reaction center from *Rhodobacter sphaeroides* R-26: Membrane–protein interactions*

(bacterial photosynthesis/membrane protein structure/membrane energetics)

T. O. YEATES†, H. KOMIYA†, D. C. REES†‡, J. P. ALLEN§, AND G. FEHER§

†University of California, Los Angeles, CA 90024; and §University of California, San Diego, La Jolla, CA 92093

Contributed by George Feher, June 2, 1987

ABSTRACT **The energetics of membrane–protein interactions are analyzed with the three-dimensional model of the photosynthetic reaction center (RC) from *Rhodobacter sphaeroides*. The position of the RC in the membrane and the thickness of the membrane were obtained by minimizing the hydrophobic energy with the energy function of Eisenberg and McLachlan. The 2-fold symmetry axis that relates the L and M subunits is, within the accuracy of 5°, parallel to the normal of the membrane. The thickness of the membrane is estimated to be 40–45 Å. Residues that are exposed to the membrane are relatively poorly conserved in the sequences of homologous RC proteins. The surface area of the RC is comparable to the surface areas of water-soluble proteins of similar molecular weight. The volumes of interior atoms in the RC are also similar to those of water-soluble proteins, indicating the same compact packing for both types of proteins. The electrostatic potential of the cofactors was calculated. The results show an asymmetry in the potential between the two possible pathways of electron transfer, with the A branch being preferred electrostatically.**

The bacterial photosynthetic reaction center (RC) is an integral membrane protein (1) composed of the three subunits L, M, and H and a number of cofactors (for a review, see ref. 2). RCs are the first membrane proteins for which three-dimensional structures are available (3–6). Whereas the structures of water-soluble globular proteins have been extensively studied, comparatively little is known about the structure and energetics of membrane proteins. We address these topics in this work.

We have examined the energetics of the membrane–protein interaction based on the three-dimensional structure of the RC from *Rhodobacter sphaeroides* (5, 6) and the hydrophobic energy function of Eisenberg and McLachlan (7). By minimizing the hydrophobic energy we determined the thickness of the membrane region and the orientation of the 2-fold symmetry axis that relates the L and M subunits with respect to the normal of the membrane. The folding of the protein was examined by calculating the volumes of buried atoms in the RC and the surface area of the RC. These two quantities were compared with those obtained for water-soluble proteins. The electrostatic potential at the cofactors has been evaluated by numerically solving Poisson's equation (8), and the possible consequences on electron transfer are discussed. A description of the structure and properties of the RC has appeared in the two preceding papers of this series (5, 6).

METHODS

The accessible surface areas of atoms in the RC structure were calculated by the method of Lee and Richards (9). This area is defined as the area of the surface traced by the center of a spherical probe as it moves over the van der Waals surface of the protein. A probe radius of 1.4 Å was used for all calculations. Volumes of buried atoms (having zero accessible surface area) were determined by the Voronoi method (10, 11).

Following Eisenberg and McLachlan (7) the hydrophobic energy, ΔG_H, was expressed as a sum involving the solvent accessible surface area of an atom, A_i, and the atomic solvation parameter, $\Delta\sigma_i$, for each atom type:

$$\Delta G_H = \Sigma\, \Delta\sigma_i A_i, \qquad [1]$$

where the sum is taken over all atoms i. ΔG_H represents the free energy of transfer of a molecule from a nonpolar solvent to water. The $\Delta\sigma_i$ are surface free energies of transfer for different atoms from a nonpolar to polar environment. The values are (in cal·Å^{-2}·mol^{-1}) (1 cal = 4.18 J): $\Delta\sigma$(C) = 16; $\Delta\sigma$(N,O) = −6; $\Delta\sigma(O^-)$ = −24; $\Delta\sigma(N^+)$ = −50; $\Delta\sigma$(S) = 21. These values were determined empirically (7) by fitting transfer free-energy data for amino acids to an energy function similar to Eq. **1**.

The electrostatic potential of the RC–membrane complex was numerically evaluated by solving the finite-difference form of Poisson's equation (8). Sources of charge density include the side chains of aspartic acid, glutamic acid, arginine, and lysine residues, the termini of each RC subunit, and half-integral charges at the ends of α-helices (12, 13). Dielectric constants for the membrane and solvent were taken to be 2 (14) and 80, respectively. Values of the protein dielectric constant varied between 4 and 20. Charge density, dielectric constants, and electrostatic potentials were sampled on a cubic grid (81 × 81 × 81), with a grid spacing of 1.5 Å. Boundary conditions of zero potential were imposed at the edges of the system.

RESULTS AND DISCUSSION

Position of the RC in the Membrane. *Theoretical considerations.* The orientation of the RC complex in the membrane cannot be directly determined from the electron density maps, since the detergent molecules that replace the membrane phospholipids during purification and crystallization are too disordered to be identified. Consequently, indirect methods must be used to delineate the interaction region between the membrane and the RC. The decrease in hydrophobic energy upon insertion of nonpolar regions of a membrane protein into a lipid bilayer provides an important driving force for protein–membrane association. We used the hydrophobic energy function (see Eq. **1**) to calculate the energy of different positions of the RC in the membrane. By systematically varying the translation and orientation of the

The publication costs of this article were defrayed in part by page charge payment. This article must therefore be hereby marked "*advertisement*" in accordance with 18 U.S.C. §1734 solely to indicate this fact.

Abbreviations: RC, reaction center; $Bchl_2$, bacteriochlorophyll dimer; Bchl, bacteriochlorophyll; Bphe, bacteriopheophytin.

*This paper is no. 3 in a series. Paper no. 2 is ref. 6, and paper no. 1 is ref. 5.

‡To whom reprint requests should be addressed.

RC in the membrane, the position of minimum energy was determined.

The above treatment makes several basic assumptions:

(*i*) The membrane may be approximated by a planar slab with uniform thickness on all sides of the RC.

(*ii*) There is a sharp interface between the membrane and the aqueous solution as well as between the RC and the membrane. These assumptions neglect, for example, other proteins (e.g., antennae) that are in contact with the RC in bacterial membranes. In addition, there is experimental support for solvent penetration into both the polar head groups and hydrocarbon regions of the membrane (14, 15), which indicates that the membrane-spanning region of the RC is not completely isolated from solvent.

(*iii*) In Eq. **1**, only hydrophobic energies are explicitly considered. Other contributions to membrane–protein energetics may also play a role. While the $\Delta\sigma_i$ values for charged oxygen and nitrogen atoms incorporate an electrostatic contribution for transfer of a charged group from an infinite nonpolar region to an infinite aqueous solution, there are boundary effects in the protein–membrane–water interactions, which introduce additional electrostatic terms. The simplest electrostatic model for a membrane consists of a planar slab of low dielectric medium immersed in a high dielectric solution. When charged groups in a high dielectric environment approach a low dielectric boundary, repulsive interactions are generated, which repel the charge from the interface. These repulsive interactions can be considered to arise from "image" charges of the same sign as the actual charge in the low dielectric region (16). These image charge interactions are reduced by decreasing the thickness of the membrane. However, decreasing the membrane thickness is unfavorable in terms of the hydrophobic interaction energy between the membrane and protein (see Fig. 2*a*). These unfavorable energetic consequences of a thinner membrane may be partially compensated by a more favorable electrostatic interaction energy between the protein and the thinner membrane. Thus, our analysis based on Eq. **1** will give an upper bound for the membrane thickness. Experimental observations on bacteriorhodopsin reconstituted into vesicles are consistent with the above ideas (17).

A measure of the extent to which the above assumptions affect the results can be obtained by comparing the membrane thickness derived from our analysis with that obtained from experiments (see later section).

Translation along the normal to the plane of the membrane. An initial estimate of the membrane spanning region of the RC was determined by evaluating ΔG_H for sections of the RC in 5-Å-thick slabs (Fig. 1). For these calculations, the slabs were sectioned normal to the local 2-fold axis (defined as the *z* axis), with the Fe atom at the origin. These values of ΔG_H provide an estimate of the free energy of transfer from the membrane to water of the surface atoms in a particular slab. A region of the RC 40–45 Å thick exhibits a large hydrophobic energy ΔG_H (Fig. 1); we conclude that this represents the membrane-spanning region.

To define more precisely the membrane-spanning region of the RC, ΔG_H was calculated for different positions of the RC in the membrane by varying both the membrane center and membrane thickness to find the position of lowest energy. Atoms that are inside the membrane for a particular position were assigned an accessible surface area of zero, while atoms outside the membrane were assigned surface areas calculated with the program of Lee and Richards (9). The normal of the plane of the membrane was initially assumed to be parallel to the *z* axis of the RC. The results of these calculations are illustrated in Fig. 2*a* for different values of membrane thickness (35 Å, 40 Å, 45 Å) as a function of the position of the membrane center along the *z* axis. The minimum value of ΔG_H decreases steeply with membrane thickness up to 40–45 Å; beyond this point, ΔG_H is relatively independent of the

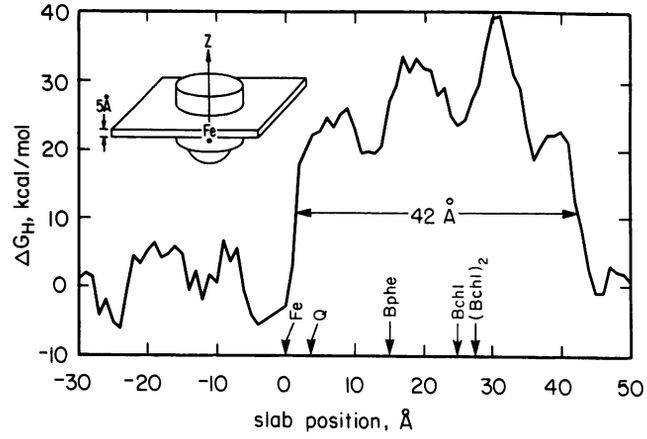

FIG. 1. The energy, ΔG_H (Eq. **1**), required to transfer a 5-Å-thick section of the RC from the membrane to water for different positions (in 1-Å increments) on the RC. The normal of the section is parallel to the 2-fold symmetry axis *z* of the RC, as indicated schematically (*Inset*). The projected locations of the centers of the cofactors onto the *z* axis are indicated. The position of the Fe was arbitrarily chosen as zero. Arrow (42 Å) indicates the membrane-spanning region. The shape of the RC (*Inset*) corresponds to a crude approximation of the RC by a cylinder 50 Å long having an ellipsoidal cross-section with minor and major radii of 20 Å and 30 Å. On one side, a hemisphere with a radius of 25 Å, corresponding to the cytoplasmic part of the H subunit, is attached. The energy calculations were performed on the experimentally determined three-dimensional structure (6).

value of the membrane thickness. Accordingly, we identify the membrane spanning region of the RC as having a thickness of 40–45 Å and centered between bacteriopheophytin (Bphe) and bacteriochlorophyll (Bchl). This value is in agreement with that obtained by sectioning the RC into slabs as discussed above.

With a membrane thickness of 40 Å, the sensitivity to vertical displacements of the RC from its lowest energy position is 1 kcal/mol for a 1-Å displacement (i.e., approximately the average thermal energy). For thinner membranes (e.g., 35 Å), the vertical position in the membrane is less accurately defined (see Fig. 2*a*), and significant translations are tolerated.

Orientation of the 2-fold symmetry axis. In the previous analysis, we translated the RC with its 2-fold symmetry axis parallel to the normal of the membrane. To test whether this corresponds to the minimum energy configuration, we varied the angle between the 2-fold axis and the normal to a 40-Å-thick membrane. The results of the dependence of G_H on the angular displacement are shown in Fig. 2*b*. From these results, we conclude that the 2-fold axis is oriented, within an estimated uncertainty of 5°, parallel to the normal of the membrane. Again, for thinner membranes the energy minimum is less pronounced (data not shown) and larger variations in angle are possible. The position of the RC in the lipid bilayer is schematically illustrated in Fig. 3.

Comparison of the membrane thickness with other data. Analysis of the hydrophobic interaction between the RC and membrane indicates that a region of 40–45 Å is isolated from exposure to water. This distance should correspond to the thickness of the membrane, including both fatty acid tails and polar head groups. Several experimental determinations of the membrane thickness have been reported. Small angle x-ray studies (19) of *Rb. sphaeroides* vesicles yield a membrane thickness of 45 ± 5 Å, in agreement with the present work. The main fatty acid component in membranes of *Rb. sphaeroides* is vaccenic acid (18:1) (20). Small angle scattering studies (21) of vesicles containing vaccenic acid indicate that the total membrane thickness of these vesicles is 38 Å, which is again similar to the distance observed in the RC

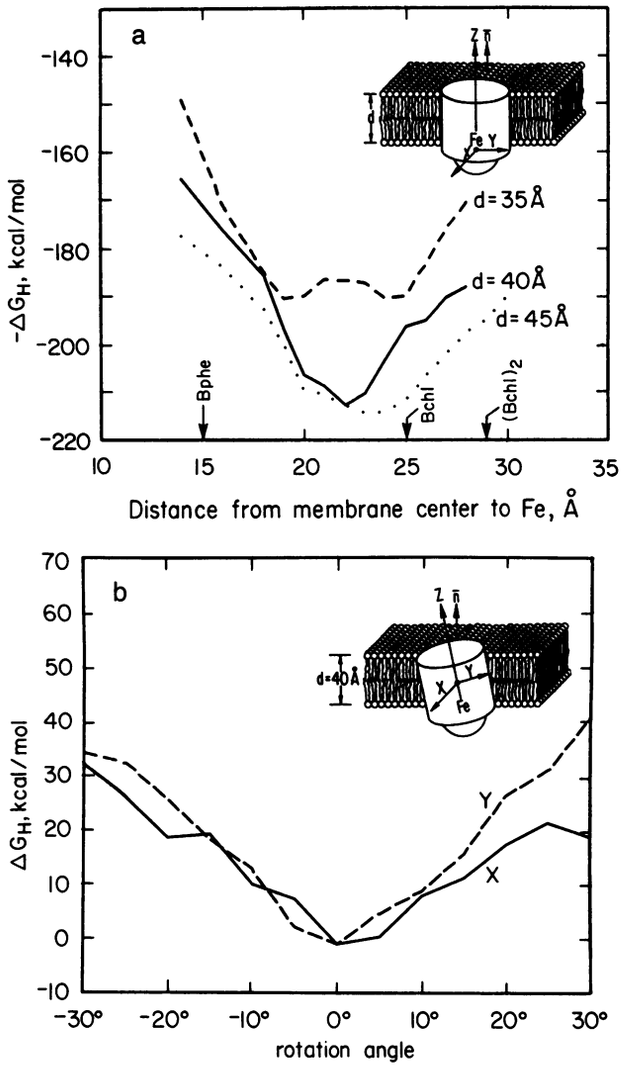

FIG. 2. (*a*) The energy, $-\Delta G_H$, required to transfer the RC from water to membrane, as a function of the position (in 1-Å increments) of the center of the membrane for different membrane thicknesses. The 2-fold symmetry axis of the RC was moved parallel to the normal of the membrane (*Inset*). The distances of the centers of cofactors from Fe along z are indicated. (*b*) Dependence of ΔG_H on rotations (in 5° increments) about axes perpendicular to the membrane normal for a 40-Å-thick membrane. The x axis is approximately along the Q_A–Q_B vector (Q_A, primary quinone; Q_B, secondary quinone), while the y axis is perpendicular to the membrane normal and the x axis. The rotation axes pass through the center of the membrane (*Inset*). The zero of energy has been chosen to correspond to a rotation angle of 0°.

work. Thus, we conclude that the assumptions made in our analysis of the energetics are basically sound.

Orientation and Position of the Transmembrane Helices. The approximate coincidence of the 2-fold axis with the normal to the membrane means that the tilt angles of the transmembrane α-helices also represent the angles between the helical axes and the membrane normal. From the data reported in ref. 6, we obtained an average tilt angle of 22° for the transmembrane helices, with the tilt angle being weighted by the number of residues forming the helix. These results are consistent with observations from polarized infrared spectroscopy studies, which indicate an average tilt angle of 20°–25° (22).

Of special interest for the structural analyses of membrane proteins is the position of the transmembrane helices in the membrane. Fig. 4 depicts the positions of the C^α atoms of the 11 transmembrane helices in the membrane. Given the helical kinks and tilts, the linear presentation in Fig. 4 distorts the

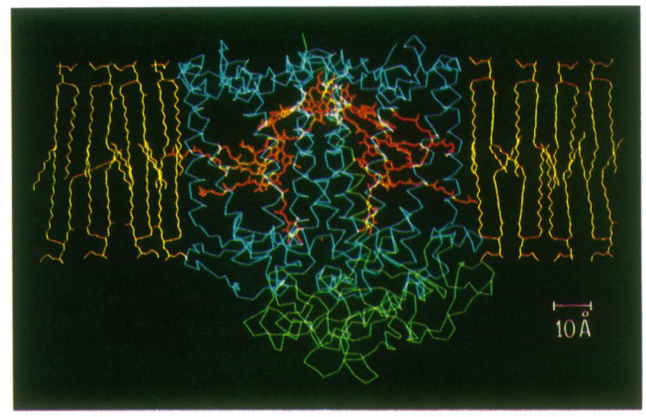

FIG. 3. Position of the RC (LM complex, blue; H subunit, green; cofactors, red) in the lipid bilayer (yellow). Structure of RC from ref. 6 (only C^α backbone shown). For simplicity, only one major type of lipid, phosphatidylethanolamine with 18:1 hydrocarbon chains is shown (for discussion of its structure, see ref. 18). Its disorder in the membrane is represented schematically. The 2-fold symmetry axis is in the plane of the paper joining the Fe (dot) near the cytoplasmic side (bottom) with the $Bchl_2$ near the periplasmic side (top).

positions by as much as ±3 Å. There is also an uncertainty of several residues in the terminal residues of each helix due to deviations from ideal hydrogen bonding and torsion angle patterns. From an analysis of the energetics discussed in the preceding section, a 40-Å-thick membrane spans the region from z = 0 Å to 40 Å in Fig. 4. The polar head-group region of the membrane has a thickness of ≈5.5 Å (14, 17)—i.e., it includes the regions with approximate z values between 0–5 Å and 35–40 Å. The nonpolar section of the membrane then extends between z = 5 Å to z = 35 Å. All the helices either completely span the nonpolar region or are within one or two residues of doing so. Over half of the helices extend beyond at least one side of the membrane–water interface. Only one helix (MB) extends beyond both interfaces.

Residues on each helix that are exposed to the membrane were identified by tabulating the accessible surface area for each residue (see *Methods*). Residues with over half of their accessible surface area exposed to the membrane are circled and hatched in Fig. 4, while residues with 20–50% of their surface area exposed to the membrane are just circled. Helices on the periphery of the RC (LA, LB, MA, MB, and HA) have more residues exposed to the membrane than helices LD and MD, which are at the center of the RC. In many instances, residues exposed to the membrane are spaced at integer multiples of three or four residues, which corresponds to the repeat distance of the α-helix. Most of the residues exposed to the membrane are nonpolar.

Fig. 4 shows that pairs of helices related by the 2-fold axis are approximately aligned (e.g., LA and MA). Furthermore, the alignment corresponds to that deduced from a sequence comparison of the L and M subunits (23). Although the coincidence of structural and sequence homologies is not surprising, Dickerson and Timkovich have described examples from the cytochrome c family where the two types of alignments are not coincident (24).

Comparison of aligned sequences (23) from *Rhodopseudomonas capsulata*, *Rb. sphaeroides*, and *Rhodopseudomonas viridis* indicates that 50% (289/580) of the residues in the L and M subunits of *Rb. sphaeroides* are conserved in all three sequences. In the transmembrane helices, sequence conservation varies with membrane exposure of the residues. Of all buried residues (with <20% membrane exposure), 59% (88/150) are conserved in all three sets of sequences. Of residues with 20–50% of their area exposed to the membrane, 42% (20/48) are conserved, while for residues with over half

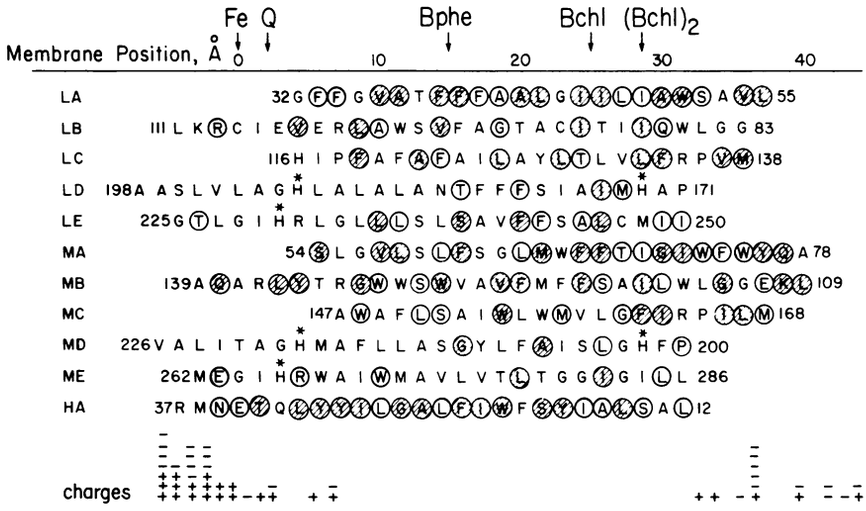

FIG. 4. Approximate positions of C^{α} atoms in the 11 transmembrane helices of the RC. Labeling of the helices follows ref. 6. (First letter refers to subunit.) Locations of the cofactors (top) and all charged residues (bottom) of the RC are indicated. Residues in hatched circles have >50% of their surface area exposed to the membrane, while residues in plain circles have 20–50% of their surface area exposed to the membrane. The remaining residues are buried inside the protein. Histidine residues marked with an asterisk are ligands to Fe or Bchl. Of the major residues in the nonpolar region, alanine is preferentially buried; phenylalanine and isoleucine are preferentially exposed to the membrane; the remaining residues show no preference. Amino acids are designated by the single-letter code.

of their area exposed to the membrane only 16% (10/62) are conserved. This suggests that fewer restrictions are placed on residues that are exposed to the membrane, implying that there are relatively few specific interactions between the RC and fatty acid chains that require the presence of specific residues. This high tolerance to substitutions of residues exposed to the membrane is reminiscent of the situation for surface residues in globular proteins; they also have a higher tolerance to substitutions than do buried residues (25).

Positions of Cofactors in the Membrane. The center of the membrane is located between the Bphes and the monomeric Bchl molecules (see Fig. 2*a*). The Fe atom and quinone rings are positioned in the region of the phospholipid head groups near the cytoplasmic side of the membrane–water interface. It should be noted, however, that both the Fe and quinone rings are surrounded by protein and cannot interact directly with the membrane. The special pair, $Bchl_2$, is located ≈10 Å below the periplasmic membrane–water interface—i.e., ≈5 Å below the polar head groups of the membrane (see Fig. 3).

Electrostatic Potential at the Cofactors. The electrostatic potential at the cofactors is expected to play an important role in the electron transfer kinetics and their pH dependence. Given the structure of the protein and the membrane, the potential can, in principle, be calculated for any point in the system. In practice, the calculations are complicated by the heterogeneous nature of the system and the unknown dielectric properties of the protein. We have calculated the electrostatic potentials at the center of the cofactors by numerically solving Poisson's equation with the finite-difference algorithm first applied to macromolecules by Warwicker and Watson (8) (see *Methods*).

The electrostatic free energy required to bring 1 mol of electrons from infinity to the center of each cofactor is plotted in Fig. 5 with respect to the distance of the cofactor from the center of the $Bchl_2$. The calculations were performed for a membrane thickness of 40 Å and with dielectric constants of 2 and 80 for the membrane and solvent. The dielectric constant of the protein, ϵ_p, was assumed to be uniform and was varied between 4 and 20. We found that for this range of values the product $\epsilon_p \cdot \Delta G_e$ (the ordinate in Fig. 5) remained invariant to within 20%.

The results of Fig. 5 show that the overall process of transferring electrons from the special pair to the primary quinone is electrostatically favorable along both branches of possible electron paths (see Fig. 5 *Inset*). However, there is an asymmetry in the potential between the two pathways, with the A branch being preferred electrostatically. For example, with $\epsilon_p = 4$, the free-energy difference between the center of the $Bchl_2$ pair and the Bphe acceptor is ≈4 kcal/mol lower along the A pathway than along the B pathway. Although it is not possible to draw quantitative conclusions about the kinetics of electron transfer from these thermodynamic considerations, the calculations identify classical electrostatic effects as a possible source of asymmetry in electron transfer kinetics between the two cofactor branches. These effects would be in addition to structural and electronic asymmetries induced by the protein–cofactor interactions.

Folding of Membrane Proteins. As a consequence of the exclusion of water from the membrane-spanning region of the RC, hydrophobic interactions do not play a major role in stabilizing the tertiary structure of this region. This is in contrast to globular water-soluble proteins. What then imparts the stability to the tertiary structure of the RC in the membrane? There are at least four types of interactions:

(*i*) *Protein structures outside the membrane-spanning region.* Several types of organized structures are observed in

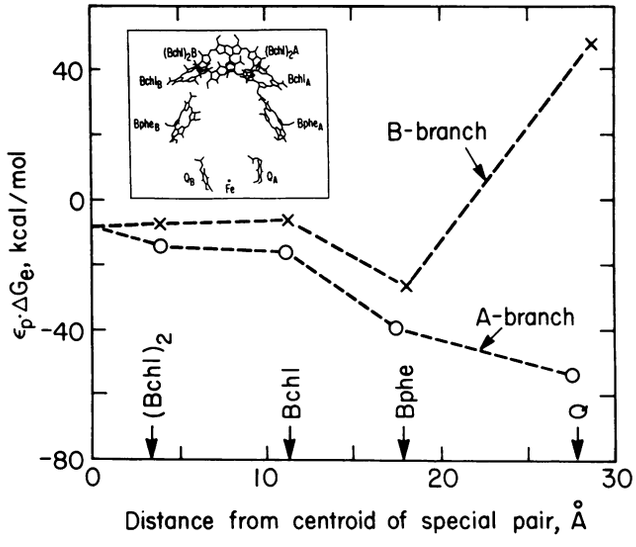

FIG. 5. Variation in electrostatic energy, ΔG_e, required to transfer 1 mol of electrons from infinity to the centers of the indicated cofactors. The energy is multiplied by the protein dielectric constant ϵ_p. This product is invariant within an accuracy of 20% for $4 < \epsilon_p < 20$. Electrostatic energies were calculated by numerical solution of Poisson's equation for a membrane thickness of 40 Å with dielectric constants of membrane and solvent of 2 and 80, respectively. (*Inset*) Two cofactor branches A and B (5). The steep increase in energy at the secondary quinone (Q_B) is due to the large number of carboxyl groups that have been assumed to be ionized. However, it is likely that most of the carboxyl groups are protonated, which would lower the energy at the Q_B position, making electron transfer from Q_A^- to Q_B possible.

the solvent exposed regions of the RC. The two periplasmic I helices (6) of the L and M subunits are suitably positioned to hold the transmembrane α-helices together on the periplasmic side. Other sections of the L and M subunits, such as the β-sheet regions, as well as contacts with the H subunit on the cytoplasmic side, may also stabilize the structure of the membrane-spanning region.

(*ii*) *Helix dipole interactions in the transmembrane region.* α-Helices exhibit a substantial dipole moment due to the nearly parallel alignment of the dipole moments of the individual peptide bonds (12, 13). Dipole–dipole energetics favor an antiparallel arrangement of interacting helices. This type of arrangement dominates the helical interactions in the membrane region of the RC. The core of the RC formed by the D and E helices of the L and M subunits is packed as a four-helical bundle (6), which imparts significant electrostatic stabilization (26).

(*iii*) *Polar interactions between transmembrane helices.* Polar interactions (including salt bridges) between helices have been proposed to stabilize the tertiary structure of the transmembrane regions of bacteriorhodopsin (27). In the RC of *Rb. sphaeroides*, however, this does not appear to be the case. On the average, less than one interhelical hydrogen bond is observed between the polar side chains of residues on different helices and no salt bridges between the membrane helices are observed. A major polar interaction that is believed to stabilize the helical arrangement is provided by the four histidine residues on the D and E helices, which form ligands to the iron atom (6).

(*iv*) *Atomic packing in the transmembrane region.* Efficient (close) packing stabilizes the tertiary structure of proteins by maximizing van der Waals contacts between atoms and minimizing the adverse consequences of cavities in the structure (28). We have calculated the volumes of buried atoms (see *Methods*) and found them to be approximately the same as those of the water-soluble proteins, carboxypeptidase (Table 1) and ribonuclease S (11) (data not shown). This suggests the same packing efficiency for both types of proteins and indicates that no significant number of detergent molecules are located inside the RC.

Another parameter that characterizes proteins is the surface/volume ratio. For the RC we calculated a surface of 35,400 Å^2 (see *Methods*). For small globular proteins (M_r, ≲30,000) the relation between surface area A (in Å^2) and M_r has been empirically determined to be $A = 11.1\ (M_r)^{2/3}$ (29). The surface area of the RC is 50% larger than predicted from this relation. However, the surface areas of proteins of M_r >30,000 have been determined to be 20–50% larger than predicted by the above relation (30). Water-soluble proteins of similar molecular weight as the RC, such as phosphorylase a, have approximately the same area as the RC.

Table 1. Volumes of buried atoms in the membrane-spanning region of the RC from *Rb. sphaeroides* and the water soluble globular protein carboxypeptidase A

	RC		Carboxypeptidase A	
Atom type	Vol, Å^3	SD, Å^3	Vol, Å^3	SD, Å^3
Main-chain atoms				
N	13	2	14	2
C^α	12	3	12	2
C	8	1	8	1
O	21	5	22	3
Pro N	9	1	10	1
Side-chain atoms				
$C^\beta H$	13	3	13	1
$C^\beta H_2$	19	4	23	8
CH	21	4	21	3
CH_2	12	2	14	2
CH_3	26	7	34	5
Aromatic C	17	5	18	5
His ring	16	5	15	4
OH	23	6	24	5
O/N	20	2	24	4
Trp	15	5	17	5

On the basis of residue hydrophobicity and volumes of buried atoms, the membrane-spanning region of the RC resembles the interior of soluble globular proteins. In contrast, the other structurally well-characterized integral membrane protein, bacteriorhodopsin, is believed to have a polar interior (27). Whether RCs and bacteriorhodopsin represent two distinct structural motifs for membrane proteins, or are simply limiting cases of a variety of intermediate cases, can only be decided as other high-resolution structures of membrane proteins become available.

We thank David Eisenberg for helpful discussions. This work was supported by grants from the National Institutes of Health (AM36053, GM13191, GM31875), the National Science Foundation (DMB85-18922, and a Presidential Young Investigators Award), and the Chicago Community Trust/Searle Scholars Program. D.C.R. is an A. P. Sloan research fellow.

1. Singer, S. J. & Nicolson, G. L. (1972) *Science* **175**, 720–731.
2. Feher, G. & Okamura, M. Y. (1978) in *The Photosynthetic Bacteria*, eds. Clayton, R. K. & Sistrom, W. R. (Plenum, New York), pp. 349–386.
3. Deisenhofer, J., Epp, O., Miki, K., Huber, R. & Michel, H. (1984) *J. Mol. Biol.* **180**, 385–398.
4. Deisenhofer, J., Epp, O., Miki, K., Huber, R. & Michel, H. (1985) *Nature (London)* **318**, 618–624.
5. Allen, J. P., Feher, G., Yeates, T., Komiya, H. & Rees, D. C. (1987) *Proc. Natl. Acad. Sci. USA* **84**, 5730–5734.
6. Allen, J. P., Feher, G., Yeates, T., Komiya, H. & Rees, D. C. (1987) *Proc. Natl. Acad. Sci. USA* **84**, 6162–6166.
7. Eisenberg, D. & McLachlan, A. D. (1986) *Nature (London)* **319**, 199–203.
8. Warwicker, J. & Watson, H. C. (1982) *J. Mol. Biol.* **157**, 671–679.
9. Lee, B. & Richards, F. M. (1971) *J. Mol. Biol.* **55**, 379–400.
10. Richards, F. M. (1974) *J. Mol. Biol.* **82**, 1–14.
11. Finney, J. L. (1975) *J. Mol. Biol.* **96**, 721–732.
12. Wada, A. (1976) *Adv. Biophys.* **9**, 1–63.
13. Hol, W. G. J. (1985) *Prog. Biophys. Mol. Biol.* **45**, 149–195.
14. Simon, S. A. & McIntosh, T. J. (1986) *Methods Enzymol.* **127**, 511–521.
15. Griffith, O. H., Dehlinger, P. J. & Van, S. P. (1974) *J. Membr. Biol.* **15**, 159–192.
16. Paul, C. H. (1982) *J. Mol. Biol.* **155**, 53–62.
17. Lewis, B. A. & Engelman, D. M. (1983) *J. Mol. Biol.* **166**, 203–210.
18. Small, M. D. (1986) *Physical Chemistry of Lipids* (Plenum, New York).
19. Pape, E. H., Menke, W., Weick, D. & Hosemann, R. (1974) *Biophys. J.* **14**, 221–232.
20. Marinetti, G. V. & Cattieu, K. (1981) *Chem. Phys. Lipids* **28**, 241–251.
21. Lewis, B. A. & Engelman, D. M. (1983) *J. Mol. Biol.* **166**, 211–217.
22. Breton, J., Deprez, J., Tavitian, B. & Nabedryk, E. (1987) in *Progress in Photosynthesis Research*, ed. Biggins, J. (Nijhoff, Dordrecht), pp. I.4.387–I.4.394.
23. Williams, J. C., Steiner, L. A. & Feher, G. (1986) *Proteins* **1**, 312–325.
24. Dickerson, R. E. & Timkovich, R. (1976) in *The Enzymes*, ed. Boyer, P. (Academic, New York), 3rd Ed., Vol. 11, pp. 397–547.
25. Smith, E. L. (1970) in *The Enzymes*, ed. Boyer, P. (Academic, New York), 3rd Ed., Vol. 1, pp. 267–339.
26. Sheridan, R. P., Levy, R. M. & Salemme, F. R. (1982) *Proc. Natl. Acad. Sci. USA* **79**, 4545–4549.
27. Engelman, D. M. & Zaccai, G. (1980) *Proc. Natl. Acad. Sci. USA* **77**, 5894–5898.
28. Rashin, A. A., Iofin, M. & Honig, B. (1986) *Biochemistry* **25**, 3619–3625.
29. Teller, D. C. (1976) *Nature (London)* **260**, 729–731.
30. Sprang, S., Yang, D. & Fletterick, R. J. (1979) *Nature (London)* **280**, 333–335.